Geological Quarterly, 2024, 68: 9
DOI: http://dx.doi.org/10.7306/gq.1737

New insights into coastal processes in the southern Baltic Sea: relevance to modelling and future scenarios

Grzegorz UŚCINOWICZ[1, *], Wojciech JEGLIŃSKI[1], Urszula PĄCZEK[1], Tomasz SZARAFIN[1], Piotr SZMYTKIEWICZ[2] and Szymon UŚCINOWICZ[2]

[1] Polish Geological Institute – National Research Institute, Kościerska 5, 80-328, Gdańsk, Poland; ORCID: 0000-0001-5185-4979 [G.U.], 0000-0002-4684-6736 [W.J.], 0000-0003-1949-1236 [U.P.], 0000-0003-1851-2840 [T.S.]

[2] Institute of Hydro-Engineering of Polish Academy of Sciences, Kościerska 7, 80-328, Gdańsk, Poland; ORCID: 0000-0001-6231-920X [P.S.], 0000-0001-6332-8546 [S.U.]

Uścinowicz, G., Jegliński, W., Pączek, U., Szarafin, T., Szmytkiewicz, P., Uścinowicz, Sz., 2024. New insights into coastal processes in the southern Baltic Sea: relevance to modelling and future scenarios. Geological Quarterly, 68: 8; https://doi.org/10.7306/gq.1737

Editor: Piotr Szrek

Understanding the relationships between shoreline changes and morpho-geological features of the seabed and hydrodynamics is important for predicting coastal dynamics. The southern Baltic barrier coast is distinguished by rhythmic shoreline features of different scales, forming an erosion-accumulation system. In this study we explore the relationships between shoreface-connected, obliquely oriented sand ridges, the distribution of wave energy, and the impact of waves on shoreline changes. A 28.5 km stretch of the Polish coast, up to 2 km offshore, was investigated using a multibeam echosounder, a sub-bottom profiler, side-scan sonar, and sediment coring. Analyses of digital terrain models, aerial photographs and maps from the late 19th century show that the boundaries between accretion and erosion zones on the coast have shifted eastwards at a rate of ~10–11 m/year. Hydrodynamic modeling shows that depressions between the ridges are "energy windows" through which higher energy waves reach the shore. The asymmetry of the ridges and their orientation relative to the prevailing wave direction suggest that they have been moving eastwards. Measurements of the ^{137}Cs content in the sediment cores show that the thickness of the dynamic layer exceeds 1.5–2.0 m. When large-scale sand ridges migrate, the "energy windows" also migrate with them, as does the entire erosion-accretion system. In conclusion, a new type of alternating shore dynamics has been identified in the dissipative, multibar southern Baltic coastal zone. It is highly likely that the average shoreline retreat measured on the scales of a few centuries and tens of kilometres may be smaller than we suspect based on observations made in recent decades.

Key words: coastal zone evolution, barrier coast, shoreface-connected sand ridges, wave energy distribution.

INTRODUCTION

Coastal barriers are one of the common features along coasts throughout the world, shielding inland basins and lowlands from the sea (e.g., Heward, 1981; Otvos, 2012; Arkema et al., 2013). Coastal erosion is thus a crucial problem for communities living on the coast (e.g., Hanson and Lindh, 1993; Zhang et al., 2002; Delle Rose, 2015). It is therefore important to recognize the conditions and factors that govern coastal development, both in terms of morphology and geology, as well as hydrodynamics, in order to reliably predict future scenarios. This knowledge is needed to use effective methods to predict coastal dynamics, as well as for spatial planning (Cooper and Mckenna, 2008; Williams et al., 2018; Uścinowicz et al., 2021). For a proper understanding of coastal development, it is necessary to understand the interaction between morphological features and hydrodynamic processes occurring not only on the beach and shoreface (*sensu* Stive and De Vriend, 1995), but within larger offshore areas. Subaqueous geological and morphological features are spatially correlated with shoreline changes at a range of temporal and spatial scales (e.g., Schupp et al., 2006).

Many studies have reported the existence of beach–surf zone interactions. Nearshore bars and their impact on sedimentological and geomorphological processes on the beach and shoreface are well recognized (e.g., Davis and Fox, 1972; Rudowski, 1986; Cohn et al., 2014). Other features, processes and phenomena, such as rip currents, associated rip channels and rip head bars, occurring on the shoreface, are also relatively well researched (e.g., Short, 1985; Rudowski, 1986; Gruszczynski et al., 1993; Brander, 1999; MacMahan et al., 2006; Schönhofer and Szmytkiewicz, 2013), but they are re-

* Corresponding author: e-mail: grzegorz.uscinowicz@pgi.gov.pl

Received: October 23, 2023; accepted: January 26, 2024; first published online: Apri 16, 2024

sponsible for shoreline changes on relatively short time scales and over tens or hundreds of metres at most.

Less known is the effect of large-scale (kilometre-long) bedforms located outside the shoreface on the shape and dynamics of the shoreline. Large-scale shoreface-connected sand ridges occur worldwide (e.g., Swift et al., 1978; McBride and Moslow, 1991; Antia, 1996). Information on their dynamics comes mainly from storm-dominated oceanic coasts and tidal seas (e.g., Short, 1992; Trowbridge, 1995; Schwab et al., 2000; Calvete et al., 2001). The results of some studies (e.g., Xu, 2015; Safak et al., 2017; Nnafie et al., 2021) indicate a spatial correlation between shoreface-connected sand ridges and shoreline undulations, leading to the hypothesis that such ridges determine the shoreline shape by modifying the waves fields. However, knowledge of the extent to which these ridges affect the large-scale (i.e., decadal and kilometre scales) morphodynamic evolution of the adjacent shoreline is limited (Nnafie et al., 2021).

Investigations carried out in recent decades on the Polish coast of the southern Baltic Sea have revealed various morphological features of varying size and stability, as well as phenomena governing coastal erosion and accumulation on different temporal and spatial scales (e.g., Furmańczyk and Musielak, 1999, 2002; Schwarzer et al., 2003). Nevertheless, only rhythmic shoreline features with dimensions of 250–400 m have been explained in terms of their origin and changes in time and space (e.g., Pruszak et al., 2008; Szmytkiewicz and Różyński, 2016). The occurrence of morphological features such as shoreface-connected sand ridges and suggestions of their possible impact on the Polish coast of the southern Baltic Sea were reported by Cieślak (1995). However, these issues have not been investigated to date. In general, the relationships between large-scale nearshore geological features and shoreline changes on the southern Baltic coast have not yet been identified.

This study investigates the relationships between large-scale offshore sand ridges oriented obliquely to the shoreface, the distribution of wave energy, and the impact of waves on the shape and position of the shoreline on the non-tidal, dissipative coast of the southern Baltic Sea.

STUDY AREA

The study area is located on the southern Baltic coast (northern Poland) and extends along a 28.5 km stretch of the coastal barrier between 17°49'13" E and 18°15'39"E, and is bounded landwards and seawards by an equidistance of 2 km from the shoreline (Fig. 1A, B). The study area is not disturbed by anthropogenic factors. The nearest breakwaters interfering with the longshore sand transport and the area of artificial beach nourishment are located in Łeba, ~15 km west of the study area.

The coast in the area of interest features a lowland in the hinterland. The surface of the lowland in the eastern part consists of wetlands at an altitude of 0.7–1.5 m a.s.l. with a network of drainage ditches, while the surface of the land in the west is slightly higher due to the aeolian sand cover.

The barrier separating the lowland and the sea is relatively narrow, with a width varying from several tens of to several hundred metres. The dune system is diverse. In general, there are low foredunes and, farther landwards, older dunes with a different morphology. The height of the dunes ranges from 5–6 m in the eastern part to 10–15 m, locally up to 30 m, in the western part. The foredune is locally absent, and erosional remnants of older and higher dunes are found directly adjacent to the beach. The width of the beach ranges from a few to several tens of metres, and its profile varies depending on the location and season. The shoreline is characterized by undulations of varying size, ranging from metres to kilometres. The largest are shoreline accretion and erosion waves (*sensu* Inman, 1987), which are rhythmic shoreline features (*sensu* Coco and Murray, 2007) with an alongshore spacing (wavelength L) of ~3–4 km and a cross-shore amplitude of ~200–300 m (Fig. 2).

The base of the shoreface (underwater coastal slope as defined by Zenkovich, 1967) is marked by a change in gradient at a depth of ~10–12 m b.s.l. The width of the slope ranges from 1.0 to 1.3 km. In the upper part of the shoreface, up to a depth of ~5–6 m, there are three to four sandbars with a relative height of ~1.0–3.5 m. Behind the shoreface, the sea depth varies between 12 and 18 m (Figs. 1B and 2A).

The study area is located within the Precambrian Platform (Znosko, 1998). Lower Proterozoic crystalline bedrock occurs in the region at a depth of ~3.2–3.3 km. Vertical crustal movements related to glacio-isostatic rebound ended in the early Holocene (Uścinowicz, 2003). Recent vertical movements of the Earth's surface range from 0 and 1 mm/year (Kontny and Bogusz, 2012; Rosentau et al., 2017).

The surface of pre-Quaternary deposits on the coast consists mainly of Miocene silts and sands with interbeds of clay and brown coal. Oligocene silt and clay occur only locally, directly beneath the Pleistocene deposits. The thickness of the Quaternary deposits is up to 40 m. The Pleistocene deposits are built of till and glaciofluvial sand, as well as of glaciolimnic sand in their uppermost part, whereas the Holocene deposits are composed of lacustrine fine sand, gyttja, and peat overlain by marine and aeolian sands (Ostaficzuk et al., 1976; Skompski, 1985).

This simple geological inland pattern continues offshore. The Pleistocene profile is dominated by calcareous glaciofluvial medium- to coarse sand and sandy gravel. Till occurs locally. Late glacial ice-marginal lake deposits (fine sand and silt), overlying the older Pleistocene deposits, occur in the north-western part of the study area. Outcrops of Pleistocene deposits occur only locally off the shoreface in the north-central part of the study area. Early Holocene lacustrine and lagoonal deposits built of fine sand with interbeds of organic matter, mud and gyttja, containing fragments of freshwater mollusc shells and peat, occur in the western part of the study area.

Middle and Late Holocene marine sand, composed mainly of quartz fine sand with an admixture of medium sand, overlies the erosional surface of Pleistocene deposits or locally of Holocene lacustrine and lagoon deposits. The erosional surface between them is clearly marked by a layer of gravel and coarse sand and/or a layer of shells. The thickness of the marine sand ranges from ~1 cm to ~8 m (Fig. 1C). The Holocene coastal evolution of the southern Baltic was strongly determined by rapid sea level rise until ~7000 yr b2k. Between 7000–5000 yr b2k the sea-level rise slowed down. Over the last 5000 years sea level has risen by ~2.5 m at an average rate ~0.5 mm/yr and the barrier has slowly migrated to its present position (Uścinowicz et al., 2007, 2022; Sydor and Uścinowicz, 2022).

The Baltic Sea is a non-tidal, storm-dominated brackish intracontinental sea. Winds from the SW, W, and NW directions dominate in the southern Baltic Sea. Storm winds (>15 m/s) and waves also tend to come from the same directions. Consequently, waves from the western sector occur in the study area for ~50% of the year. Waves from the NE, E, and SE occur for 32% of the year, and those from N for 13.5% of the year. The height of waves is usually 0.5–1.5 m (47% of the year). According to multi-year data, the periods of mean waves (T_{mean}) vary from 3 to 7.5 s, and the periods of the significant waves (T_s) during heavy storms exceed 9 s. The following wave parameters

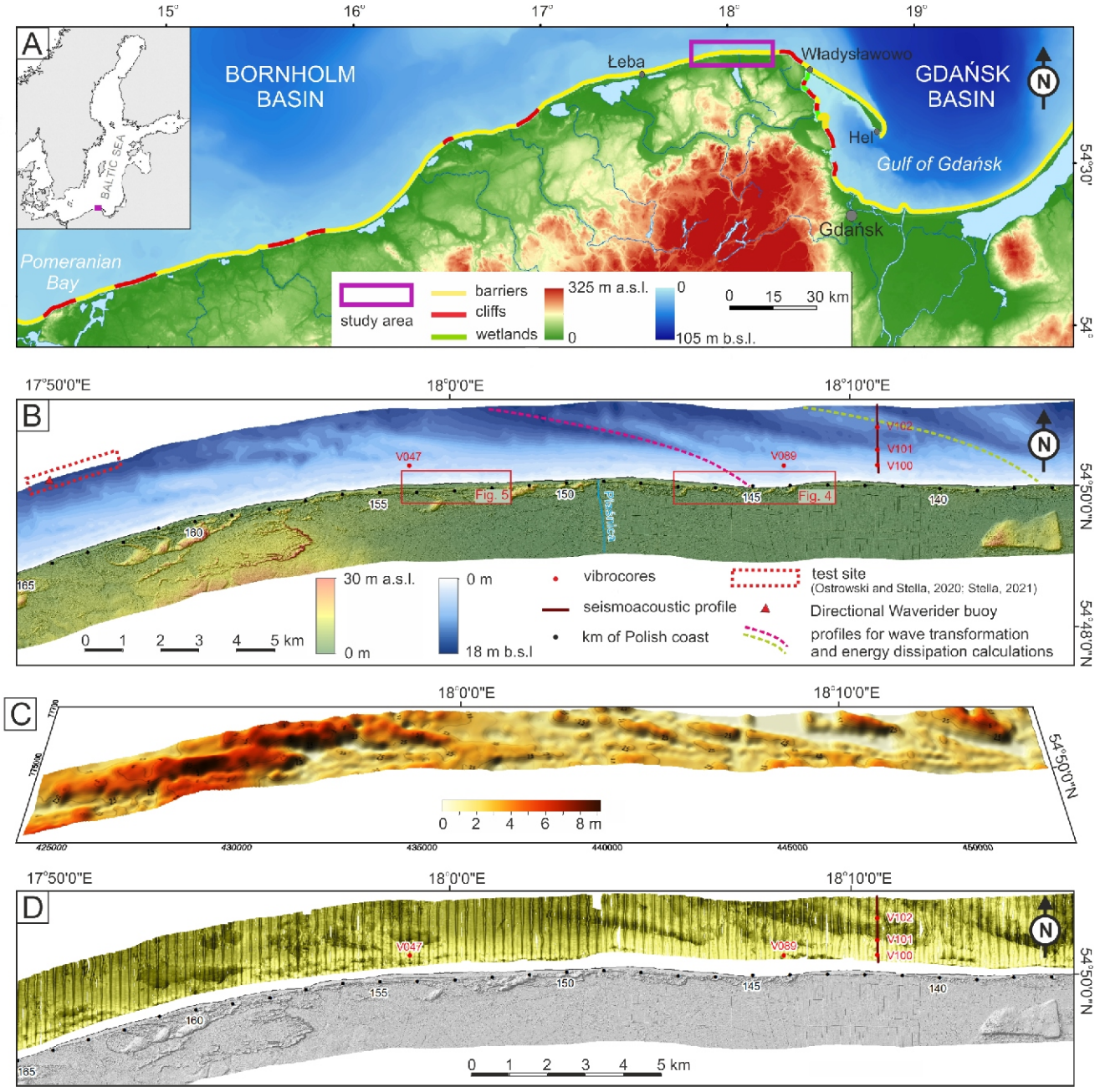

Fig. 1. Location and characterization of the study area

A – location of the study area; **B** – DTM and location of the seismoacoustic profile and sediment cores, the test site of repeated bathymetric and side-scan sonar (SSS) mapping and directional waverider buoy are located in NW part of the study area, profiles for calculations of wave transformation and energy dissipation are shown by red and green dashed lines; **C** – 3D model of marine sand thickness, the thickness of the marine sand in the ridges ranges between 4 and 8 m whereas within depressions it is <1 m; **D** – SSS mosaic, dark tones indicate coarse sand and gravel occurring in the depressions between the sandy ridges

were recorded during the hurricane on 6 December 2013: H_{max} = 7.8 m, H_s = 4.42 m, H_{mean} = 2.8 m, T_s = 9.3 s, T_{mean} = 8.1 s (Ostrowski et al., 2016).

The annual resultant (net) longshore sediment transport on the upper shoreface is ~111,000–145,000 m^3/year, moving from west to east (Szmytkiewicz et al., 2021). According to the nearest mareographic stations in Łeba and Władysławowo, the maximum water level during the migration of low air pressure systems and associated storm surges can reach 1.68 m and 1.38 m above the average (Wiśniewski et al., 2009). According to the mareographic station located in Władysławowo (~10 km west of the study area), the average rate of sea level rise between 1951 and 2015 was 2.04 mm/year (Kowalczyk, 2019).

MATERIALS AND METHODS

FIELDWORK

Measurements were carried out along profiles parallel and perpendicular to the shoreline at intervals ensuring full coverage of the seabed. Bathymetric measurements were performed

Fig. 2. Eagle-eye view of rhythmic shoreline features; the erosional and accretionary areas and the transitional zone (nodal point) in the eastern part of study area (~144.5–141.0 km of Polish coast; source: PGI-NRI data, photo M. Olkowicz)

using a multibeam sonar system (*Geoswath GS4*+, Kongsberg – frequency versions: 500 kHz), and a seismoacoustic survey was carried out using a sub-bottom profiler (*Meridata HD* SBP – chirp transducer, 2–9 kHz). As a result of seismoacoustic profiling, the geological structure of the area was identified to a depth of ~20 m b.s.b. (below sea bottom). Side-scan sonar profiling was carried out using a *SonarTech Side Scan Sonar S-150* with a frequency of 400 kHz and a maximum range of 140 m. 122 sediment cores, each ~3 m long, were collected using a vibrocorer *VKG-03/04*, as well as 130 sediment grab samples. The *GPS RTK Trimble SPS-461* navigation system was used, with a position accuracy better than 0.5 m.

LABORATORY ANALYSIS

The cores and surface sediment samples were described in macroscopic detail, and samples for analysis were collected from each layer according to macroscopically visible differences in grain size. Grain size analysis at 1 unit intervals was performed by sieving for sand and gravel, and by the laser diffraction method using a *Malvern Laser Mastersizer 3000* for silty and clayey sediments. In addition, when the content of grains <0.063 mm was found to be equal to or greater than 10% of the sample after sieving, its composition was also determined by the laser method. Laser diffraction analyses were carried out after removing organic matter from the sediments using 30% hydrogen peroxide (H_2O_2).

Measurements of ^{137}Cs activity were performed on 16 samples from two cores. The measurements were carried out by gamma-ray spectrometry. All samples were first dried in a dryer at 60°C until their mass was constant. The samples were then thoroughly mixed and homogenized and placed in tightly sealed 0.65 dm^3 Marinelli beakers. The ^{137}Cs isotope activity was measured on the basis of a 661.7 keV gamma peak. The detection limit was equal to 0.5 Bq/kg. IAEA-375 reference (distributed by the Laboratory of Seibersdorf IAEA, Vienna, Austria) was used as a standard of ^{137}Cs activity. The ^{137}Cs activities in the samples were decay-corrected to the date of sampling, and the result was expressed in Bq/kg.

DATA POST-PROCESSING AND SPATIAL ANALYSIS

Post-processing of survey results was performed using *MERIDATA MDPS* software. This resulted in a digital terrain model (DTM) with a resolution of 5 5 m, a bathymetric map and a side-scan sonar mosaic. Interpretation of seismoacoustic data supported by core profile data was also performed.

Spatial analyses were performed using German topographic maps at a scale of 1:25,000 from 1875 (Messtischblatter: 135-Wittenberg, 136-Dembek, 137-Ostrau), as well as aerial photographs from 1958, 1996, and 2020. A DTM based on airborne LIDAR scanning conducted in 2009 and 2020 was also analyzed.

SCOPE AND METHODS OF HYDRODYNAMIC MODELLING

Calculating wave parameter transformations, taking into account wave refraction, wave-bottom friction and wave breaking were done using the method described and introduced by Bowen (1969) and summarised by Battjes and Janssen (1978). In Poland, this method was first applied and described by Szmytkiewicz et al. (2000), then adopted and reproduced by Pruszak et al. (2008) as well as Szmytkiewicz et al. (2021).

Assuming no wave reflections from the shore and no interactions between the current and wave dynamics, the equation for the conservation of energy flux for parallel isobaths simplifies to the following form:

$$\frac{}{x} \; E \; C_g \; \cos \quad D \; 0 \qquad [1]$$

where: – the angle between the wave ray and the line perpendicular to the shore; C_g – the group velocity of the wave; D – the wave energy dissipation; E – the total wave energy.

Assuming that the wave height at each point in the nearshore zone, including the surf zone, can be described by the Rayleigh distribution, the dissipation of wave motion energy is expressed by the formula proposed by Battjes and Janssen (1978):

$$D \quad \frac{}{4} \; Q_b \; f_p \quad g \; H_m^2 \qquad [2]$$

where: – an empirical coefficient of order 0(1); Q_b – a factor characterizing the percentage of breaking waves at a given depth in the nearshore zone; $f_p \quad \frac{1}{T_p}$ – the frequency of the wave spectrum peak; – water density; g – gravitational acceleration, H_m – maximum allowable wave height at a given point in the nearshore zone.

For shallow water ($k \quad h \quad 0$) we have:

$$H_m \quad h \qquad [3]$$

where: – the wave refraction coefficient; h – water depth at a given point.

For the southern Baltic Sea, based on a series of measurements, it has been established that = 0.8 for stormy conditions and = 0.55 for average wave conditions.

For waves whose height is described by the Rayleigh distribution, the energy can be determined using the equation:

$$E \quad \frac{1}{8} \quad g \; H_{rms}^2 \qquad [4]$$

where: H_{rms} 113 $\overline{H}$ (the root mean square wave height); $\overline{H}$ – the average wave height.

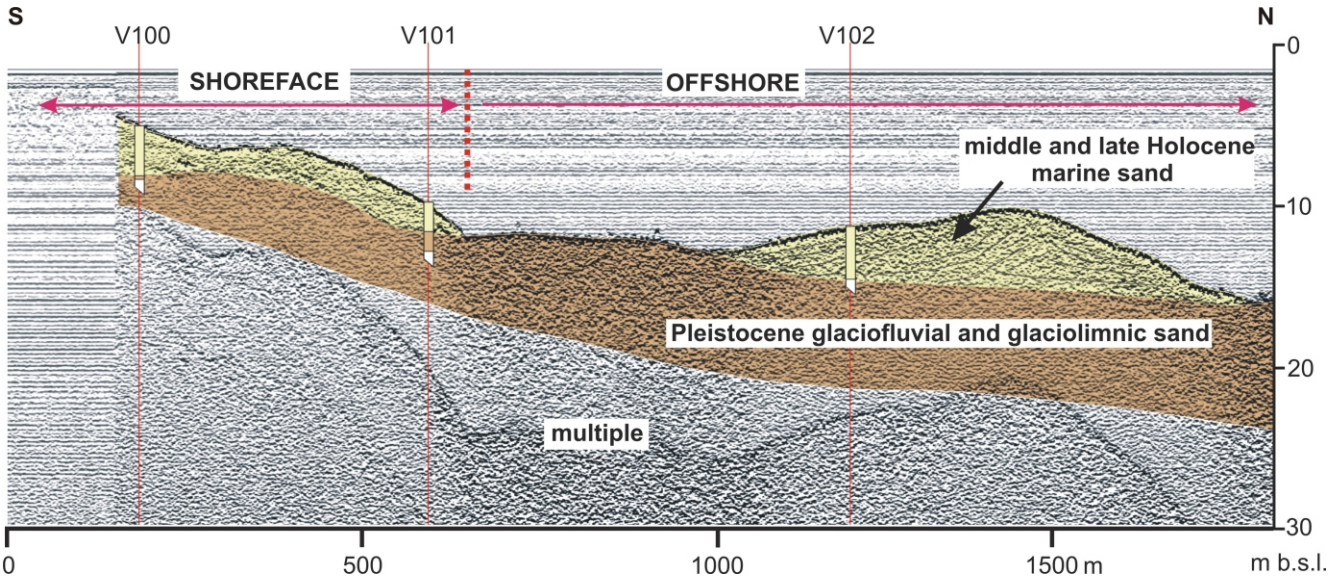

Fig. 3. Interpreted seismoacoustic profile across a sand ridge

Location of the profile is shown on Figure 1B

By substituting the expressions for energy dissipation due to the breaking process into the energy conservation equation, we obtain:

$$\frac{1}{8} \quad g \frac{}{x} \quad H_{rms}^2 \quad C_g \quad \cos \quad \frac{}{4} \quad Q_b \quad f_p \quad g \quad H_m^2 \quad 0 \qquad [5]$$

The wave heights at each point in the coastal zone are calculated from the Equation 5.

Despite significant simplifications in describing the mechanism of breaking waves, this model has gained general approval and is widely used to this day. Practically, all commercial numerical packages (*Delft3D*, *Mike 21* and others) are based on this approach. From the long-term experiences of various researchers, including the authors of this study, it is found that the error in calculating the wave heights approaching the shore does not exceed 10% (Komar 1998, Booij et al., 1999).

RESULTS AND INTERPRETATION

Seabed mapping showed a series of shoreface-connected sand ridges occurring at depths of 12 to 18 m and oriented obliquely to the shoreface,. The distance between the crests of the ridges varies between ~0.7 and 1.2 km, and their relative height is ~4–6 m (Figs. 1B, C and 3). The distance between the extremities of the ridges (measured parallel to the shoreline) amounts to ~3–4 km, which is close to the alongshore spacing (L) of shoreline waves. The ridges are slightly asymmetrical, with steeper slopes facing NE. They are built of fine- and medium-grained quartz sand containing shells of marine molluscs. The thickness of coarse and gravelly sand in the depressions between the ridges does not exceed 0.5 m. Outcrops of glacial till and glaciofluvial sand occur locally (Figs. 1D and 3).

The thickness of the contemporarily mobile layer of sand, transported by currents and waves during storms, was determined by measuring the content of ^{137}Cs in the cores. Caesium

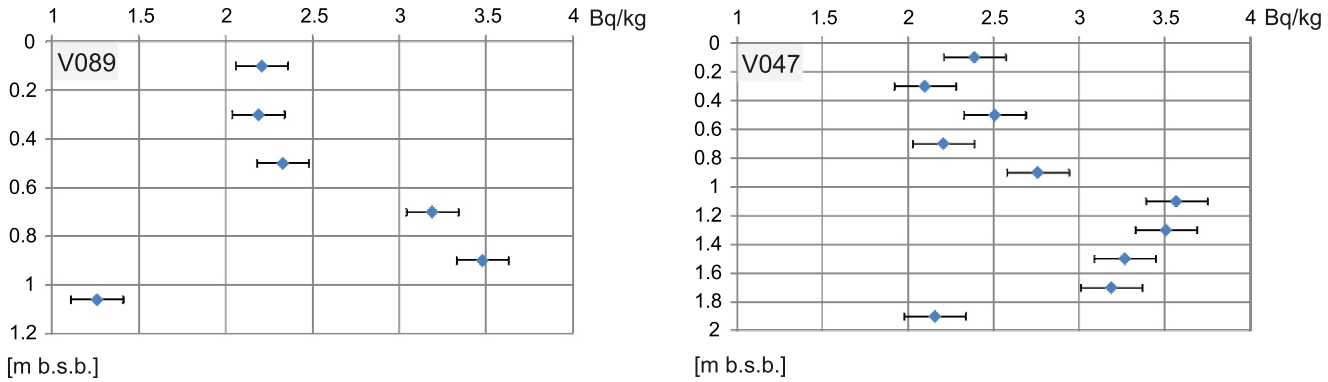

Fig. 4. ^{137}Cs content in the sands of cores V047 and V089

Location of the profile is shown on Figure 1B

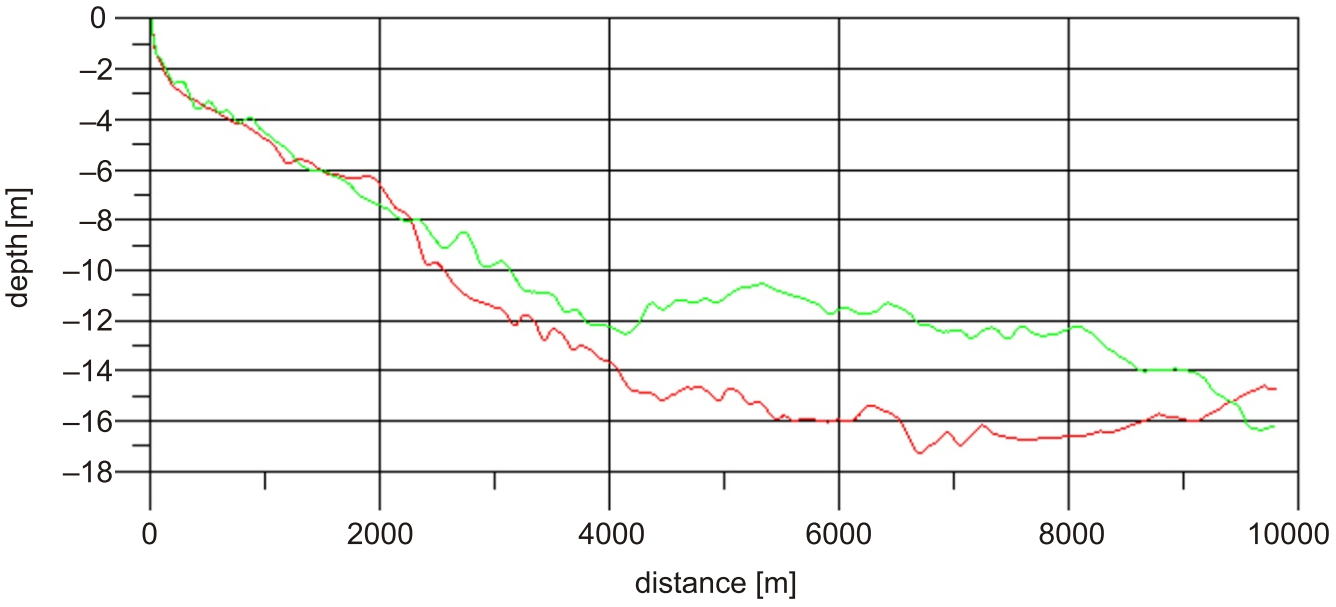

Fig. 5. Seabed profiles for which wave transformation and energy dissipation calculations were performed

The red profile is located along the axis of the depression between ridges, the green profile is located along the axis of ridge; location of the profiles is shown on Figure 1B

137 is an artificial radionuclide, which entered the environment after 1945 as a result of nuclear weapons testing and accidents in nuclear power plants. Therefore the presence of caesium in sandy deposits allows the determination of the thickness of the layer undergoing redeposition during the last few decades. The content of ^{137}Cs in marine sand within the study area was recorded to a depth of more than 1.18 m b.s.b. in core V089 taken at 14.7 m water depth and 2.0 m b.s.b. in core V047 taken at 10.2 m water depth (Fig. 4). Although the cores were collected in relatively shallow water, ^{137}Cs is known from other surveys to occur up to 2 m below the seabed surface in cores taken at water depths of up to 25 m (Bojanowski et al., 1996; Uścinowicz et al., 2014, 2019).

Shoaling of seabed topography towards the shore affects wave transformation, which leads to wave breaking, which in turn generates longshore currents, followed by mass transport of sediments. As the seabed relief is heterogeneous the wave field is also heterogeneous. The transformation of a sample storm wave and the amount of energy dissipated during wave breaking were calculated for two profiles; the first located along the depression between ridges and the second along the ridge axis (Fig. 1B). The observed differences in depth over a distance of ~4,000 to 8,500 m are in the range of 4 to 5 m (Fig. 5).

On Figure 6 the calculated transformation of a sample stormy wave approaching the shore with a height of H_s = 4 m is shown (H_s = 4 m is a typical wave height during strong storms in

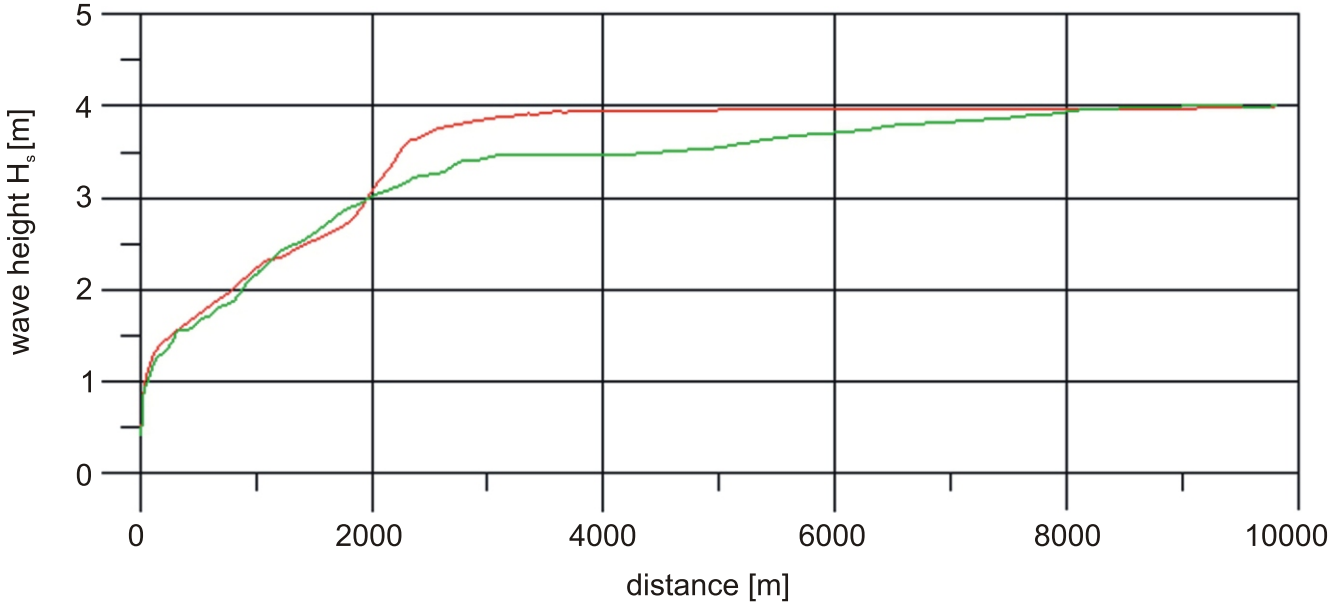

Fig. 6. Wave height transformation along a depression between ridges (red line) and along a ridge axis profile (green line)

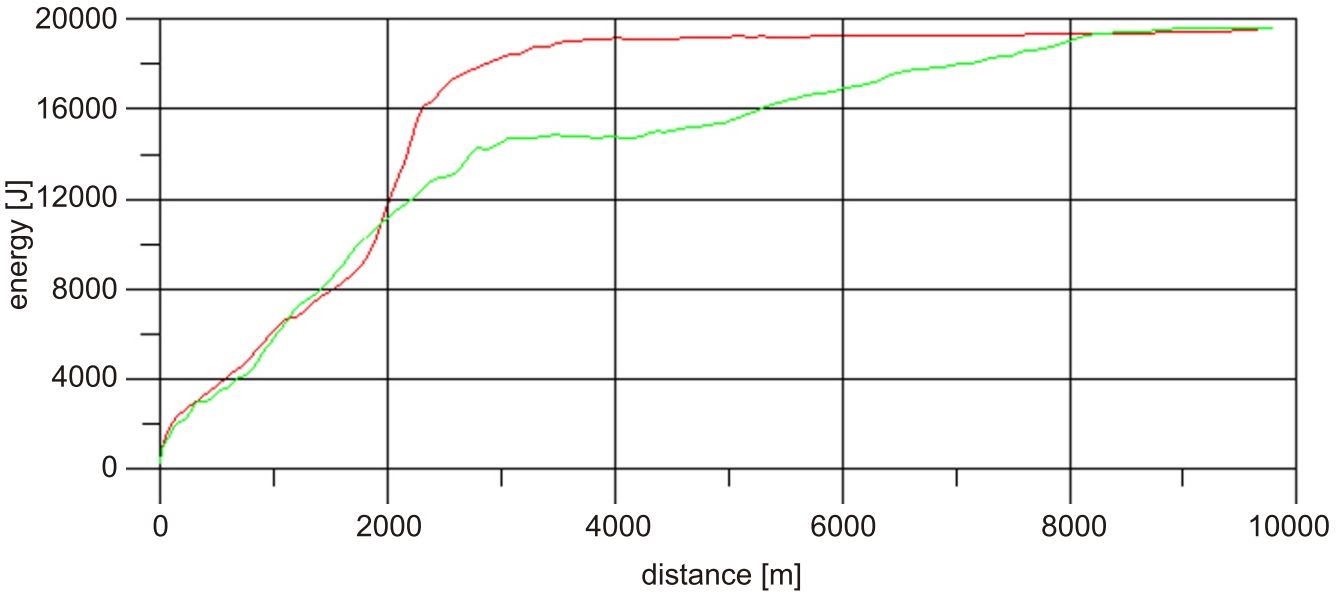

Fig. 7. Wave energy transformation along a depression between ridges (red line) and along the ridge axis profile (green line)

this region; see Cerkowniak et al., 2014). From this figure it can be seen that in the profile along the depression between ridges, at a distance of ~4,000 m from the shore, the wave still maintains a height of 4 m, while in the along-ridge axis profile, the wave has already decreased to a height of 3.5 m. This seemingly small difference in wave height translates into significant energy values.

Figure 7 shows the calculated wave energy along the profiles, while Figure 8 illustrates the difference in energy quantity between the two profiles. It can be observed that in the profile along a depression between ridges, the wave energy is ~4,000 J higher than in the profile along the ridge axis. Therefore we called depressions between the ridges "energy windows". Such a substantial amount of energy must result in increased coastal erosion in the profile along depressions between ridges. The substantial energy in these windows is expected to result in increased coastal erosion along the profiles within these depressions.

Another aspect deserves attention. The differences in wave heights within and outside the energy window are depicted in Figure 7, specifically in the region traditionally known as the "beyond surf zone" (Stella et al., 2019). Comparing wave heights from ~6000 m to ~3000 m from the shore, wave heights within the energy window are ~30% higher. This suggests that, at this distance from the shore, beyond the region of bars, the occurrence of higher waves and greater bottom orbital velocities significantly intensifies processes causing erosion of surface sediments within the energy windows. Conversely, in the nearshore area within the surf zone (bars), wave heights are similar, indicating that lithodynamic processes are comparable within and outside the energy window. This observation may imply more substantial wave erosion of the sand cover on the seabed outside the sandbar areas, subsequently leading to more pronounced erosion (due to a deficit of sand on the underwater slope) of the coastal area (beach).

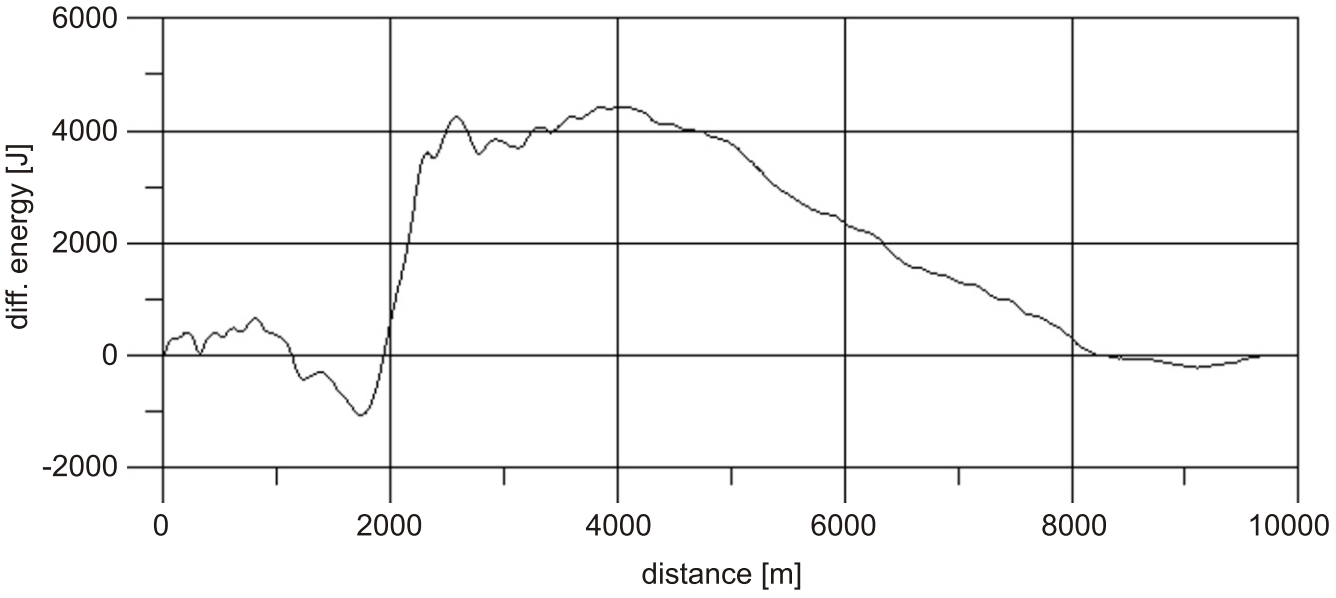

Fig. 8. Differences between the wave energy along a depression between ridges and along the ridge axis profile

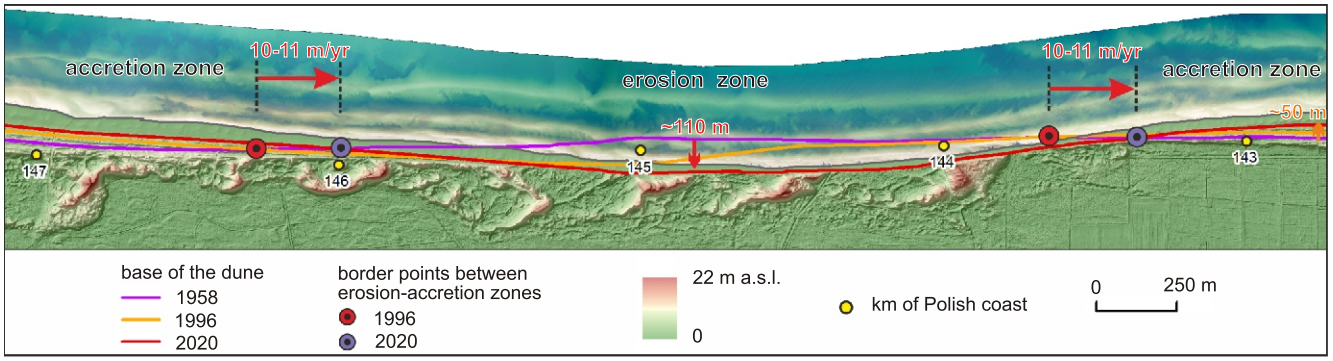

Fig. 9. Migration of erosional and accretionary zones in the years 1996–2020 based on air photos (1958 and 1996 and LIDAR DTM 2020)

Background: land – LIDAR DTM 2020; sea – air photo 2020

The calculations presented were performed for a single storm wave. In real conditions, such storms occur for several to several tens of hours during one storm event and ~5 times a year. Assuming that major storms last ~10 hours and occur ~5 times a year, with storm waves having a period of ~10 seconds and significant wave height of ~4 m, on average (Ostrowski et al., 2016), there is ~72 MJ/year more energy in the nearshore area of the beach and dunes. This lead to more significant beach and dune reshaping in areas that are aligned with the "energy windows". As a result of the variation in wave energy reaching the shore, rhythmic erosional and accretion shoreline patterns are formed (Figs. 2, 9 and 10).

It is crucial to highlight an additional significant aspect: the similarity between a specific characteristic of the wave climate and the geometry of the underwater ridges (energy windows) identified. On the open sea, particularly in the Baltic proper, storm waves commonly propagate from west to east. The process of wave refraction in the ocean causes waves, when closer to the shore (typically at depths of around 30–40 m in the conditions of the South Baltic), to start "sensing" the seabed. As a result, they change their direction of propagation from west to north-west, and in the nearshore area, they reach the shore in a north-northwest direction. The shape of underwater ridges (energy windows) roughly corresponds to the shape of storm wave rays. This implies that storm waves play a crucial role in the dynamics of the generating and reshaping of the structures analyzed. In this context, other processes, such as e.g. water level fluctuations, do not appear to be directly associated with the phenomenon discussed.

The asymmetry of the sand ridges and their orientation in relation to the prevailing winds, and thus the direction of the waves, suggest that they are moving eastwards. The presence of ^{137}Ce proves sand redeposition in recent decades. The high dynamics of the seabed are also confirmed by modeling of hydro- and lithodynamic processes (Ostrowski and Stella, 2020) and detailed bathymetric and side-scan sonar surveys (Stella, 2021) carried out at a test site near the study area (Fig. 1B). Theoretical modeling shows that the joint impact of waves and currents under storm conditions can cause intense motion of sandy sediments. Bathymetric and side-scan sonar surveys (Stella, 2021) revealed that the seabed elevation changed by a maximum of 0.7 m in one year, and sand waves (with a wave length of 50–100 m) shifted by a maximum of ~20 m.

The present data lead to the conclusion that the sand ridges outside the shoreface are migrating, along with "energy windows", and consequently the whole system of shoreline accretion and erosion waves on the coast is also migrating. This means that the position of large-scale rhythmic shoreline fea-

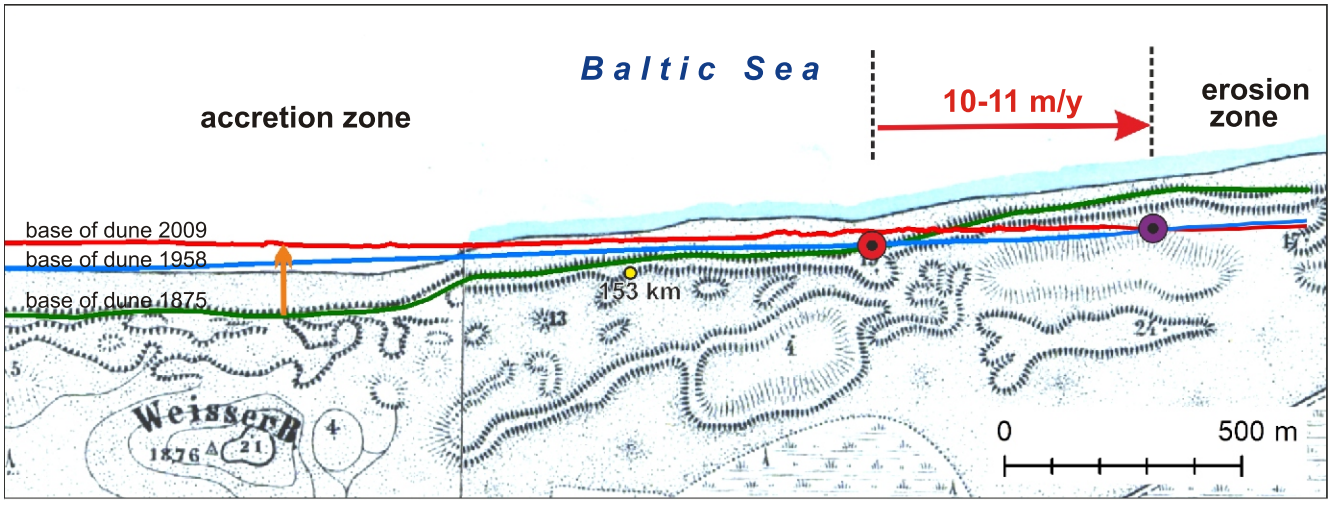

Fig. 10. Migration of erosional and accretionary zones in the years 1958–2009 based on a topographic map from 1875 (background), an air photo from 1958 and a LIDAR DTM of 2009

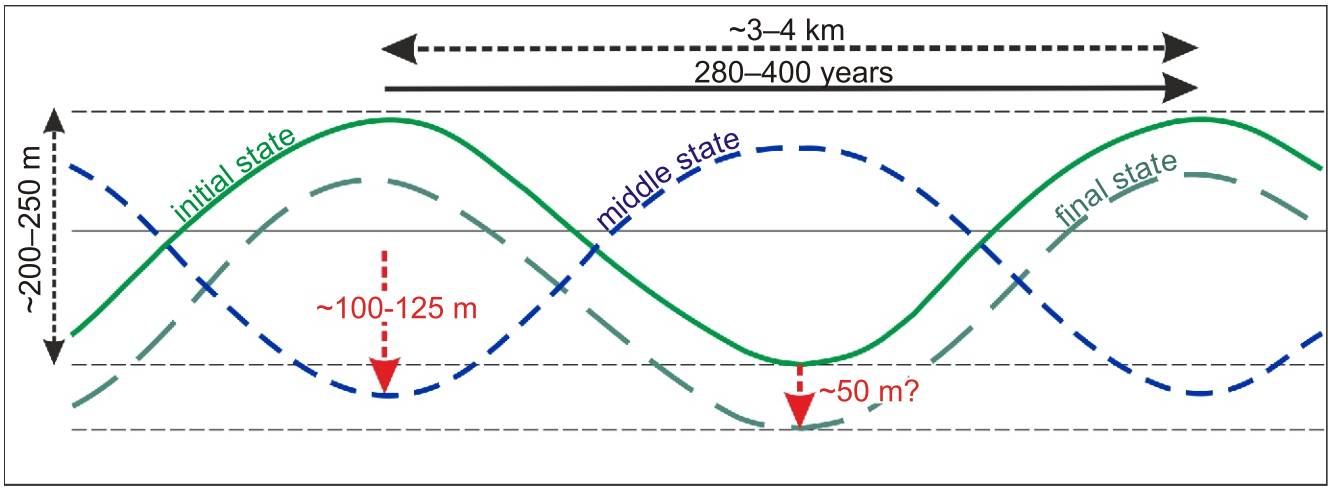

Fig. 11. Conceptual model of how the southern Baltic coastal zone functions on a centennial scale

tures is not constant over time. To determine the migration rate of shoreline accretion and erosion waves along the coast, measurements of the position of border (nodal) points were carried out in different periods. Measurements based on aerial photographs from 1958, 1996 and 2020 show that the migration rate between 1996 and 2020 amounted to ~10–11 m/year (Fig. 9). Comparison of a topographic map from 1875, aerial photographs from 1958 and the DTM from 2009 gave the same rate of migration for the period 1958-2009 (Fig. 10).

DISCUSSION

Predictions of coastal evolution on a decadal (short) time scale were made based on the assumption that erosion and accretion zones do not change their position (e.g., Deng et al., 2017; Uścinowicz and Szarafin, 2018). Similarly, some studies (e.g., Xu, 2015; Safak et al., 2017) indicating correlations between shoreface-connected sand ridges and the shoreline shape suggest, based on the historical shoreline record, that shoreline undulations are persistent. Nnafie et al. (2021) stated, however, that knowledge of the extent to which these ridges affect the large-scale (i.e., decadal and kilometre scales) morphodynamic evolution of the adjacent shoreline, and vice versa, is limited.

This study proposes a coastal evolution model in which erosion and accretion zones, i.e. shoreline undulations, migrate along the shore. Given the migration rate of rhythmic shoreline features revealed in this study, it takes ~140–200 years for the erosion zone to be replaced by the accumulation zone. This means that after ~280–400 years the shoreline can assume its former shape and position, but only if there has been no loss of sand within the sandbar, beach and foredune areas. In fact, during storms, some of the sand is transported by cross-shore currents via gaps in the bars outside the shoreface. The range of these processes is poorly understood. A rough estimation based on differences between the range of erosion and accretion of dunes and beaches in adjacent areas during the same period suggests that up to ~40–60% of the sand is lost. Nevertheless, even if a certain amount of sand never returns to the beach, the average shoreline retreat measured on the scale of centuries and tens of kilometres is smaller than we believe based on observations and measurements on the scale of decades, or less than half a cycle at the most (Fig. 11).

In this context, the view of persistent shoreline undulations associated with shoreface-connected sand ridges seems to be justified only if the studies analyzed relatively short-term shoreline records, e.g. “historical” (Xu, 2015) or 50-year records (Safak et al., 2017), and did not account for the migration of ridges and did not analyze the positions of nodal points on the shore. We present an alternative model based on the analysis of changes in the location of nodal points, where, under the hydrodynamic conditions of the southern Baltic, kilometre-scale changes in shoreline undulations should be considered on a centennial scale.

The migration rate of rhythmic shoreline features calculated in this study applies to a relatively short period of a few decades. If the rate of coastal changes depends on the migration rate of offshore sand ridges, then the dynamics of these mega-scale bedforms is a crucial issue. We can assume that the migration rate of bedforms and, consequently, the migration rate of rhythmic shoreline features, depend on changes in hydro-meteorological conditions on different time scales. When the frequency of storms increases or decreases, for example, as a result of North Atlantic Multidecadal Oscillations (e.g., Bärring and Fortuniak, 2009; Börgel et al., 2020), or over longer periods of time (e.g., Goslin et al., 2018; Pouzet et al., 2018; Uścinowicz et al., 2022), the rate and range of seabed dynamics and associated coastal processes also change.

Nevertheless, although there is little information on the seabed dynamics of the southern Baltic Sea and their possible changes over time, the results presented here indicate that the range and rate of changes of the coast depend on the migration rate of shoreface-connected ridges, their orientation relative to the coast, and the prevailing directions of waves.

The findings presented here come from a thoroughly investigated but relatively short section of the Polish Baltic coast, so the question arises as to whether they also apply to a larger section of the coast, or is this a purely local phenomenon? Shoreline undulations and associated erosion and accretion areas of varying sizes are common features along the Polish coast. However, there is very little comprehensive data on seabed morphology to directly correlate shoreline undulations with seabed features located offshore, i.e. behind the shoreface, and associated differences in the wave energy approaching the shore. The best explored area, apart from the one presented in this paper, is the coast of the Hel Peninsula and the adjacent seabed north of the peninsula. Shoreline undulations and asso-

ciated erosion and accretion zones were investigated along a stretch of several kilometres of the NW section of the Hel Peninsula (e.g., Furmańczyk, 1994; Zawadzka, 1999; Stachurska, 2012). Behind the shoreface in that area, there are several-kilometre-long sand ridges and depressions in between, oriented obliquely to the coast (Gajewski et al., 2004; Łęczyński et al., 2007), and the landward extremities of the depressions are strictly correlated with the erosional sections of the coast. Hydrodynamic modeling showed a correlation between seabed relief and energy approaching the shore. Lithodynamic modeling revealed also significant seabed dynamics (Łęczyński et al., 2007; Łęczyński, 2009). Despite the published data, there is no certainty as to the origin of the ridges, whether they are relict forms, such as remnants of former spits from the transgression period, or whether they are large-scale sand ridges formed recently by current hydrodynamics. With regard to shoreline undulation, due to the long (>150 years) history of coastal protection works on the Hel Peninsula, natural coastal processes are strongly disturbed and it is not possible to track changes in the positions of nodal points between erosion and accretion areas. However, it can be expected that the conceptual model presented can be applied to some other sections of the Polish coast, or even on a larger scale – to the southern and southeastern coast of the Baltic Sea, in areas where large volumes of sand occur on the lower shoreface and offshore, which allows the formation of sand ridges. The same may be true of storm-dominated ocean coasts, as well as tidal sea coasts. However, it should be borne in mind that the rate of the processes discussed may be different than in the epicontinental and tideless Baltic Sea.

CONCLUSIONS

The results presented here help explain the relationship between oblique shoreface-connected ridges and corresponding shoreline changes. The location of shoreline accretion and erosion waves on beaches depends on geological, geomorphological and hydrodynamic factors. It has been shown that depressions between shoreface-connected sand ridges are "energy windows" through which more wave energy can reach the coast. Particularly, in this study, calculations of wave transformation and energy dissipation were carried out for the first time for the southern Baltic Sea area to determine how much more energy reaches the shore through "energy windows". The results obtained indicate that, in the case of a single storm wave, ~4,000 J more energy reaches the shore through "energy windows" than in adjacent areas. If the average statistical year is considered, this difference amounts to 72 MJ/year. As a result, shoreline erosion and accretion waves *sensu* Inman (1987) develop onshore. Large-scale offshore ridges are slowly shifted by dominant currents, and the "energy windows" migrate with them as well, so that the entire erosion-accretion system that forms kilometre-long rhythmic shoreline features also migrates. Although some sand is transported beyond the shoreface and incorporated into the offshore system of ridges at the base of the shoreface, the average shoreline retreat measured on the scale of centuries and tens of kilometres may be smaller than we suspect based on observations and measurements performed over recent decades. To conclude, a new type of alternating shore dynamics has been identified in the dissipative, multibar southern Baltic coastal zone. The changes identified have been taking place for hundreds of years and extend over tens of kilometres along the shore. These new findings should be considered when exploring coastal zone dynamics and developing predictive engineering models, as well as long-term coastal protection plans. It could have also a significant impact on the design of new, naturally based methods for coastal protection in the southern Baltic Sea region in the future.

Acknowledgements. The authors acknowledge receipt of the following financial support for the research and publication of this article: the data were collected as part of the project "4D cartography in the coastal zone of the southern Baltic Sea" funded by the National Fund for Environmental Protection and Water Management. The editorial work was supported by mission-related funds of the Polish Geological Institute – National Research Institute (project 62.9012.2022.00.0).

REFERENCES

Antia, E.E., 1996. Shoreface-connected ridges in German and US Mid-Atlantic Bights: Similarities and contrasts. Journal of Coastal Research, **12**: 141–146; https://www.jstor.org/stable/4298468

Arkema, K.K., Guannel, G., Verutes, G., Wood, S.A., Guerry, A., Ruckelshaus, M., Kareiva, P., Lacayo, M., Silver, J.M., 2013. Coastal habitats shield people and property from sea-level rise and storms: Nature Climate Change, **3**: 913–918; https://doi.org/10.1038/nclimate1944

Battjes, J.A., Janssen, J.P.F.M., 1978. Energy loss and set-up due to breaking of random waves. Proceedings of 16th International Conference on Coastal Engineering, **1**: 569–587.

Bowen, A.J., 1969. The generation of longshore currents on a plane beach. Journal of Marine Research, **27**: 206–215.

Bärring, L., Fortuniak, K., 2009. Multi-indices analysis of southern Scandinavian storminess 1780–2005 and links to interdecadal variations in the NW Europe–North Sea region. International Journal of Climatology, **29**: 373–384; https://doi.org/10.1002/joc.1842

Bojanowski, R., Radecki, Z., Uścinowicz, Sz., Knapińska-Skiba, D., 1996. Penetration of caesium –137 into sandy sediments of the Baltic Sea. Proceedings of the Baltic Marine Science Conference, Rønne, Denmark, ICES Cooperative Research Report, No. **257**: 85–89.

Booij, N., Ris, R.C., Holthuijsen, L.H., 1999. A third-generation wave model for coastal regions. 1. Model description and validation. Journal of Geophysical Research, **104**: 7649–7666; https://doi.org/10.1029/1998JC900123

Börgel, F., Frauen, C., Neumann, T., Meier, H.E.M., 2020. The Atlantic multidecadal oscillation controls the impact of the North Atlantic oscillation on North European climate. Environmental Research Letters, **15**: 104025; https://doi.org/10.1088/1748-9326/aba925

Brander, R.W., 1999. Field observations on the morphodynamic evolution of a low-energy rip current system. Marine Geology, **157**: 199–217; https://doi.org/10.1016/S0025-3227(98)00152-2

Calvete, D., Falques, A., de Swart, H.E., Walgreen, M., 2001. Modelling the formation of shoreface-connected sand ridges on storm-dominated inner shelves. Journal of Fluid Mechanics, **441**: 169–193; https://doi.org/10.1017/S0022112001004815

Cerkowniak, G., Ostrowski, R., Szmytkiewicz, P., 2014. Climate change related increase of storminess near Hel Peninsula, Gulf of Gdańsk, Poland. Journal of Water and Climate Change, **6**: 300–312.

Cieślak, A., 1995. Contemporary coastal transformation – the coastal management and protection aspect. Journal of Coastal

Research, Special Issue: **22**, 63–71; https://www.jstor.org/stable/25736029

Coco, G., Murray, A.B., 2007. Patterns in the sand: From forcing templates to self-organization. Geomorphology, **91**: 271–290; https://doi.org/10.1016/j.geomorph.2007.04.023

Cohn, N., Ruggiero, P., Ortiz, J., Walstra, D.J., 2014. Investigating the role of complex sandbar morphology on nearshore hydrodynamics. Journal of Coastal Research, Special Issue, **66:** 53–58; https://doi.org/10.2112/SI65-010.1

Cooper, J.A.G., Mckenna, J., 2008. Working with natural processes: The challenge for coastal protection strategies. The Geographical Journal, **174**: 315–331; https://doi.org/10.1111/j.1475-4959.2008.00302.x

Davis, R.A., Jr., Fox, W.T., 1972. Coastal processes and nearshore sand bars. Journal of Sedimentary Petrology, **42**: 401–412; https://doi.org/10.1306/74d72568-2b21-11d7-8648000102c1865d

Delle Rose, M., 2015. Medium-term erosion processes of south Adriatic beaches (Apulia, Italy): a challenge for an integrated coastal zone management. Journal of Earth Science & Climatic Change, **6**, 306; https://doi.org/10.4172/2157-7617.1000306

Deng, J., Harff, J., Zhang, W., Schneider, R,. Dudzińska-Nowak, J., Giza, A., Terefenko, P., Furmańczyk, K., 2017. The dynamic equilibrum shore model for the reconstruction and future projection of coastal morphodynamics. Coastal Research Library, **19**: 271–287; https://doi.org/10.1007/978-3-319-49894-2_1

Furmańczyk, K., 1994. Present coastal zone development of the tide less sea in light of the South Baltic Sea coast remote sensing investigating (in Polish with English summary). Uniwersytet Szczeciński Rozprawy i Studia, (**235) 161**.

Furmańczyk, K., Musielak, S., 1999. Circulation systems of the coastal zone and their role in south Baltic morphodynamic of the coast. Circulation systems of the coastal zone and their role in the South Baltic morphodynamics of the coast. Quaternary Studies in Poland, Special Issue: 91–94.

Furmańczyk, K., Musielak, S., 2002. Important features of coastal dynamics in Poland: „Nodal Points" and „Gates". In: Baltic coastal ecosystems. Structure, Function and Coastal Zone Management (Ed. G. Schernewski and U. Schiwer): 141–147, Springer-Verlag Berlin, Heidelberg, New York; https://doi.org/10.1007/978-3-662-04769-9

Gajewski, L., Gajewski, Ł., Rudowski, S., Stachowiak, A., 2004. The relief of the offshore sea bottom at Karwia-Chałupy Polish Baltic coast. Polish Geological Institute Special Papers, **11**: 91–94.

Goslin, J., Fruergaard, M., Sander, L., Gałka, M., Menviel, L., Monkenbusch, J., Thibault, N., Clemmensen, L.B., 2018. Holocene centennial to millennial shifts in North-Atlantic storminess and ocean dynamics. Scientific Reports, **8**: 1–12; https://doi.org/10.1038/s41598-018-29949-8

Gruszczyński, M., Rudowski, S., Semil, J., Słominski, J., Zrobek, J., 1993. Rip currents as a geological tool. Sedimentology, **40**: 217–236; https://doi.org/10.1111/j.1365-3091.1993.tb01762.x

Hanson, H., Lindh, G., 1993. Coastal erosion: an escalating environmental threat. Ambio, **22**: 188–195.

Heward, A.P., 1981. A review of wave-dominated clastic shoreline deposits. Earth-Science Reviews, **17**: 223–276; https://doi.org/10.1016/0012-8252(81)90022-2

Inman, D.L., 1987. Accretion and erosion waves on beaches. Shore & Beach, **55**: 61–66.

Komar, P.D., 1998. Beach Processes and Sedimentation, 2nd Edition, Prentice Hall, Upper Saddle River, New Jersey 07458: 544.

Kontny, B., Bogusz, J., 2012. Models of vertical movements of the earth crust surface In the area of Poland derived from leveling and GNSS data. Acta Geodynamica et Geomaterialia, **9**: 331–337.

Kowalczyk, K., 2019. Changes in mean sea level on the Polish coast of the Baltic Sea based on tide gauge data from the years 1811–2015. Acta Geodynamica et Geomaterialia, **16** : 195–209; https://doi.org/10.13168/AGG.2019.0016

Łęczyński, L., 2009. Morpholithodynamics of the Hel Peninsula coastal zone (in Polish with English summary). Wydawnictwo Uniwersytetu Gdańskiego, Gdańsk.

Łęczyński, L, Chlebus, N, Grusza G., Jędrasik, J., 2007. Morphologic and hydrodynamic conditions of Hel Peninsula's abrasion in the Kuźnica region (southern Baltic). Oceanological and Hydrobiological Studies, **36**: 21–37; https://doi.org/10.2478/v10009-007-0006-5

MacMahan, J.H., Thornton, E.B., Reniers, J.H.M., 2006. Rip current review. Coastal Engineering, **53**: 191–208; https://doi.org/10.1016/j.coastaleng.2005.10.009

McBride, R.A., Moslow, T.F., 1991. Origin, evolution, and distribution of shoreface sand ridges, Atlantic inner shelf, U.S.A. Marine Geology, **97**: 57–85; https://doi.org/10.1016/0025-3227(91)90019-Z

Nnafie, A., de Swart, H.E., Falqués, A., Calvete, D., 2021. Long-term morphodynamics of a coupled shelf-shoreline system forced by waves and tides, a model approach. Journal of Geophysical Research: Earth Surface, **126**, e2021JF006315; https://doi.org/10.1029/2021JF006315

Ostaficzuk, S., Jakubicz, B., Skompski, S., 1976. Szczegółowa mapa geologiczna Polski w skali 1:50 000, arkusz Sławoszyno (in Polish). Państwowy Instytut Geologiczny, Warszawa.

Ostrowski, R., Stella, M., 2020., Potential dynamics of non-tidal sea bed in remote foreshore under waves and currents. Ocean Engineering, **207**: 1–6; https://doi.org/10.1016/j.oceaneng.2020.107398

Ostrowski, R., Schönhofer, J., Szmytkiewicz, P., 2016. South Baltic representative coastal field surveys, including monitoring at the Coastal Research Station in Lubiatowo, Poland. Journal of Marine Systems, **162**: 89–97; https://doi.org/10.1016/j.jmarsys.2015.10.006

Otvos, E.G., 2012. Coastal barriers — Nomenclature, processes, and classification issues. Geomorphology, **139–140**: 39–52; https://doi.org/10.1016/j.geomorph.2011.10.037

Pouzet, P., Maanan, M., Piotrowska, N., Baltzer, A., Stephan, P., Robin, M., 2018. Chronology of Holocene storm events along the European Atlantic coast: new data from the Island of Yeu, France. Progress in Physical Geography: Earth and Environment, **42**: 431–450; https://doi.org/10.1177/0309133318776500

Pruszak, Z., Różyński, G., Szmytkiewicz, P., 2008. Megascale rhythmic shoreline forms at a beach with multiple bars. Oceanologia, **50**: 183–203.

Pruszak, Z., Szmytkiewicz, P., Ostrowski, R., Skaja, M., Szmytkiewicz, M., 2008. Shallow-water wave energy in a multi-bar coastal zone. Oceanologia, **50**: 43–58.

Rosentau, A., Bennike, O., Uścinowicz, Sz., Miotk-Szpiganowicz, G., 2017. The Baltic Sea Basin. In: Submerged Landscapes of the European Continental Shelf: Quaternary Paleoenvironments (ed. N.C. Flemming, J. Harff, D. Moura, A. Burgess and G. Bailey): 103–133. Wiley-Blackwell.

Rudowski, S., 1986. Sedimentary environment at the barred coast of a tideless sea; Southern Baltic, Poland. Studia Geologica Polonica, **87**: 1–76.

Safak, I., List, J. H., Warner, J.C., Schwab, W.C., 2017. Persistent shoreline shape induced from offshore geologic framework: effects of shoreface connected ridges. Journal of Geophysical Research: Oceans, **122**: 8721–8738; https://doi.org/10.1002/2017JC012808

Schönhofer, J., Szmytkiewicz, M., 2013. Identification of rip currents in the coastal zone of the southern Baltic – modeling and observations in nature (in Polish with English summary). Inżynieria Morska i Geotechnika, **6**: 505–515.

Schupp, C.A, McNinch, J.E., List, J.H., 2006. Nearshore shore-oblique bars, gravel outcrops, and their correlation to shoreline change. Marine Geology, **233**: 63–79; https://doi.org/10.1016/j.margeo.2006.08.007

Schwab, W.C., Thieler, E.R., Allen, J.R., Foster, D.S., Swift, B.A., Denny, J.F., 2000. Influence of inner-continental shelf geologic framework on the evolution and behavior of the barrier-island system between Fire Island Inlet and Shinnecock Inlet, Long Is-

land, New York. Journal of Coastal Research, **16**: 408–422; https://www.jstor.org/stable/4300050

Schwarzer, K., Diesing, M., Larson, M., Niedermeye, R.-O., Schumacher, W., Furmanczyk, K., 2003. Coastline evolution at different time scales - examples from the Pomeranian Bight, southern Baltic Sea. Marine Geology, **194**: 79–101; https://doi.org/10.1016/S0025-3227(02)00700-4

Short, A.D., 1985. Rip currents type, spacing and persistence, Narrabeen Beach, Australia. Marine Geology, **65**: 47–71; https://doi.org/10.1016/0025-3227(85)90046-5

Short, A.D., 1992. Beach systems of the central Netherlands coast: Processes, morphology and structural impacts in a storm driven multi-bar system. Marine Geology, **107**: 103–137; https://doi.org/10.1016/0025-3227(92)90071-O

Skompski, S., 1985. Szczegółowa mapa geologiczna Polski w skali 1:50 000, arkusz Choczewo (in Polish). Instytut Geologiczny, Warszawa.

Stachurska, B., 2012. Analysis of changes in the position of the sea-side coast of Hel Peninsula based on aerial photographs from the years 1947-1991 (in Polish with English summary). Inżynieria Morska i Geotechnika, **4**: 542–553.

Stella, M., 2021. Morphodynamics of the south Baltic seabed in the remote nearshore zone in the light of field measurements. Marine Geology, **439**: 106546; https://doi.org/10.1016/j.margeo.2021.106546

Stella, M., Ostrowski, R., Szmytkiewicz, P., Kapiński, J., Marcinkowski, T., 2019. Driving forces of sandy sediment transport beyond the surf zone. Oceanologia, **61**: 50–59; https://doi.org/10.1016/j.oceano.2018.06.003

Stive, M.J.F., De Vriend, H.J., 1995. Modelling shoreface profile evolution. Marine Geology, **126**: 235–248; https://doi.org/10.1016/0025-3227(95)00080-I

Swift, D.J.P., Parker, G., Lanfredi, N.W.,Perillo, G., Figge, K., 1978. Shoreline-connected sand ridges on American and European shelves - a comparison. Estuarine, Coastal and Shelf Science, **7**: 227–247.

Sydor, P., Uścinowicz, Sz., 2022. Holocene relative sea-level changes in the eastern part of Pomeranian bay and the Szczecin Lagoon, Southern Baltic Sea. The Holocene, **32**: 351–368; https://doi.org/10.1177/09596836221074028

Szmytkiewicz, P., Różyński, G., 2016. Infragravity waves at a dissipative shore with multiple bars: recent evidence. Journal of Waterway, Port, Coastal and Ocean Engineering, **142**: 04016007.

Szmytkiewicz, P., Szmytkiewicz, M., Uścinowicz, G., 2021. Lithodynamic processes along the seashore in the area of planned nuclear power plant construction: a case study on Lubiatowo at Poland. Energies, **14**: 1636; https://doi.org/10.3390/en14061636

Trowbridge, J.H., 1995. A mechanism for the formation and maintenance of shore-oblique sand ridges on storm-dominated shelves. Journal of Geophysical Research, **100** (C8): 16071–16086; https://doi.org/10.1029/95jc01589

Uścinowicz, G., Szarafin, T., 2018. Short-term prognosis of development of barrier-type coasts (Southern Baltic Sea). Ocean and Coastal Management, **165**: 258–267; https://doi.org/10.1016/j.ocecoaman.2018.08.033

Uścinowicz, G., Szarafin, T., Pączek, U., Lidzbarski, M., Tarnawska, E., 2021. Geohazard assessment of the coastal zone – the case of the southern Baltic Sea. Geological Quarterly, **65**: 5; https:// doi.org/10.7306/gq.1576

Uścinowicz, Sz., 2003. The Southern Baltic relative sea level changes, glacio-isostatic rebound and shoreline displacement. Polish Geological Institute Special Papers, **10**: 1–79.

Uścinowicz, Sz., Zachowicz, J., Miotk-Szpiganowicz, G., Witkowski, A., 2007. Southern Baltic sea-level oscillations: New radiocarbon, pollen and diatom proof of the Puck Lagoon. GSA Special Paper, **426**: 143–158; https://doi.org/10.1130/2007.2426(10)

Uścinowicz, Sz., Jegliński, W., Miotk-Szpiganowicz, G., Nowak, J., Pączek, U., Przezdziecki, P., Szefler, K., Poręba, G., 2014. Impact of sand extraction from the bottom of the southern Baltic Sea on the relief and sediments of the seabed. Oceanologia, **56**: 857–880; https://doi.org/10.5697/oc.56-4.857

Uścinowicz, Sz., Adamiec, G., Bluszcz, A., Jegliński, W., Jurys, L., Miotk-Szpiganowicz, G., Moska, P., Pączek, U., Piotrowska, P., Poręba, G., Przezdziecki, P., Uścinowicz, G., 2019. Chronology of the last ice sheet decay on the southern Baltic area based on dating of glaciofluvial and ice-dammed lake deposits. Geological Quarterly, **63** (1): 192–207; https://doi.org/10.7306/gq.1453

Uścinowicz, Sz., Cieślikiewicz, W., Skrzypek, G., Zgrundo, A., Goslar, T., Jędrysek, M.-O., Jurys, L., Koszka-Maroń, D., Miotk-Szpiganowicz, G., Sydor, P., Zachowicz, J., 2022. Holocene relative water level and storminess variation recorded in the coastal peat bogs of the Vistula Lagoon, southern Baltic. Quaternary Science Reviews, **296**: 107782; https://doi.org/10.1016/j.quascirev.2022.107782

Williams, A.T., Rangel-Buitrago, N., Pranzini, E., Anfuso, G., 2018. The management of coastal erosion. Ocean & Coastal Management, **156**: 4–20; https://doi.org/10.1016/j.ocecoaman.2017.03.022

Wiśniewski, B., Wolski, T., Kowalewska-Kalkowska, H., Cyberski, J., 2009. Extreme water level fluctuations along the Polish coast. Geographia Polonica, **82**: 99–107; https://doi.org/10.7163/GPol.2009.1.9

Xu, T., 2015. Wave transformation and alongshore sediment transport due to obliquely oriented shoreface-connected ridges. Doctoral dissertation, Georgia Institute of Technology. Retrieved from http://hdl.handle.net/1853/54466

Zawadzka, E., 1999. Development tendencies of the Polish shores of the southern Baltic Sea (in Polish with English summary). Gdańskie Towarzystwo Naukowe, Gdańsk.

Zenkovich, V.P., 1967. Processes of Coastal Development. Edinburgh: Oliver and Boyd.

Zhang, K., Douglas, B., Leatherman, S., 2002. Do storms cause long-term beach erosion along the U.S. East Barrier Coast? The Journal of Geology, **110**: 493–502; https://doi.org/10.1086/340633

Znosko, J., (ed.), 1998. Atlas tektoniczny Polski (in Polish). Państwowy Instytut Geologiczny, Warszawa.